Journal of Atmospheric and Terrestrial Physics, Vol. 54, No. 3/4, pp. 467–477, 1992.
Printed in Great Britain.

0021-9169/92 $5.00 + .00
Pergamon Press plc

Plasmaspheric wind

J. LEMAIRE* and R. W. SCHUNK

Center for Atmospheric and Space Science, Utah State University, Logan, UT 84322-4405, U.S.A.

(*Received in final form* 1 *August* 1991)

Abstract—Observational evidence is presented indicating that beyond $L = 1.7$–2 plasma corotating in the plasmasphere expands continuously with a small outward directed bulk velocity perpendicular to geomagnetic field lines. A numerical simulation of plasmaspheric flux tube drift motion is presented in support of such an outward plasma expansion. The maximum expansion velocity inside the plasmasphere is determined by the maximum value of the plasma interchange velocity, which is inversely proportional to the value of the integrated Pedersen conductivity.

1. INTRODUCTION

The plasmasphere is a toroidal shaped region surrounding the Earth that extends out to a distance of 4–5 Earth radii in the equatorial plane of the magnetosphere. This region is populated with a relatively high density, cold plasma of ionospheric origin. This plasma is basically trapped on closed geomagnetic field lines and corotates with the Earth. However, at low latitudes, wind-induced dynamo electric fields can cause an additional plasma drift across the geomagnetic field, while at high latitudes magnetospheric electric fields can lead to non-corotational cross-B drifts.

In the early 1960s, the plasmasphere was frequently observed to have a sharp outer edge, where the density can decrease by two orders of magnitude in a fraction of an Earth radius (CARPENTER, 1963; GRINGAUZ, 1963). This sharp 'knee' in the equatorial density distribution is associated with the plasmapause, which is the outer boundary of the plasmasphere. Subsequently, this boundary was found both to display a marked longitudinal asymmetry, with a distinct bulge in the dusk sector (CARPENTER, 1970), and to be a sensitive function of geomagnetic activity (CARPENTER and PARK, 1973; CHAPPELL, 1972). Because of its dependence on geomagnetic activity, the formation of the plasmapause was attributed to magnetospheric convection (NISHIDA, 1966; BRICE, 1967), whereby substorm enhanced electric fields act to peel away the relatively dense outer plasmasphere in the post-midnight local time sector. However, LEMAIRE (1985) suggested that the sharp density gradients at the plasmapause could be caused by plasma drifts associated with the interchange instability. Nevertheless, it is now well established that during prolonged periods of very quiet geomagnetic conditions, the equatorial plasmapause can be smooth and can be at a geocentric distance beyond 6.6 Earth radii (R_E), while during very active conditions it can have a sharp knee at a distance as close as 3 R_E.

During the last 30 years, the dynamics and energetics of the plasmasphere have been extensively modelled. The studies that have been conducted cover a wide range of topics, including the diurnal variation of the plasmasphere (MAYR *et al.*, 1972; BAILEY *et al.*, 1973), the plasmasphere's ability to maintain the nocturnal ionosphere (MOFFETT and MURPHY, 1973; MURPHY *et al.*, 1976), the effects of electromagnetic drifts on the plasmasphere (MURPHY *et al.*, 1980; RASMUSSEN and SCHUNK, 1990), the mechanisms responsible for the formation of the light ion trough (BAILEY *et al.*, 1978), the conditions leading to H^+–O^+ and H^+–He^+ counterstreaming on plasmaspheric field lines (BAILEY *et al.*, 1977; YOUNG *et al.*, 1980; RICHARDS *et al.*, 1983), the effect of the geomagnetic tilt on interhemispheric coupling (RICHARDS and TORR, 1986; GUITER *et al.*, 1991), and the mechanisms leading to detached plasma elements (GREBOWSKY and CHEN, 1976; LEMAIRE, 1985). Also, numerous studies have been conducted of plasmaspheric refilling characteristics after depletion induced by geomagnetic substorms. These studies considered the effect on the refilling rate due to Coulomb collisions, wave–particle interactions, shocks, and electromagnetic drifts (see BANKS *et al.*, 1971; SCHULZ and KOONS, 1972; KHAZANOV *et al.*, 1984; SINGH *et al.*, 1986; RASMUSSEN and SCHUNK, 1988; LEMAIRE, 1989a; WILSON *et al.*, 1990; and references therein).

In this paper we discuss a mechanism that was originally proposed by LEMAIRE (1985) for the con-

*On leave of absence from the Institut d'Aéronomie Spatiale de Belgique, Brussels, Belgium.

tinual loss of plasma from the plasmasphere. This loss mechanism, which has not been included in any of the above studies, corresponds to a subsonic outflow of cold plasma corotating in the geomagnetic field and contained in the gravitational potential well. This so-called 'plasmaspheric wind' results from a plasma interchange motion that is driven by an imbalance between gravitational, centrifugal, and pressure gradient forces. The maximum interchange velocity (wind velocity) is determined by the height-integrated Pedersen conductivity in the ionosphere. The wind should exist at all times, even during prolonged periods of quiet geomagnetic conditions when substorm disturbances are absent. In presenting arguments in support of this hypothesis, we first review the arguments presented by LEMAIRE (1985) and then provide additional supporting information. However, conclusive proof of the existence of the plasmaspheric wind requires a co-ordinated effort involving multi-instrument *in-situ* measurements of plasmaspheric parameters like those envisaged during the future REGATTA mission.

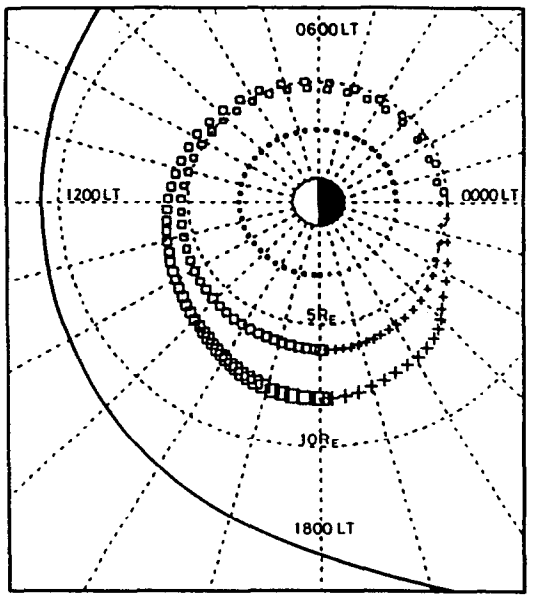

Fig. 1. Drift paths of three plasma elements in MCILWAIN's (1974) electric and magnetic field distributions E3H and M2, respectively. The symbols indicate their successive positions each 30 min interval of time. The size of the symbols changes along the drift path to indicate the variation of the equatorial cross-section. The type of symbol representing a given plasma element changes when it traverses the midnight meridional plane (0000 LT). The radial distance for the three drift paths is maximum in the dusk local time sector, at 8, 6 and 3 R_E. Note the large dawn–dusk asymmetry of the two outer trajectories (after LEMAIRE, 1985).

2. QUIET TIME PLASMASPHERE REFILLING CHARACTERISTICS

Our emphasis is on the dynamics of the plasmasphere during a prolonged quiet period following a depletion induced by a substorm. We discuss a range of topics, including the drift paths of flux tubes during quiet times, the evolution of equatorial densities during refilling, refilling times, the diurnal variation of nearly full flux tubes, and the variation of the equatorial density with L during quiet times. The calculations associated with these topics support our hypothesis that a plasmaspheric wind exists. Measurements are also presented which support this hypothesis.

2.1. *Equatorial drift paths of plasmaspheric flux tubes*

The calculation of the motion of plasma elements in the plasmasphere requires a knowledge of the electric and magnetic field distributions. For steady and low geomagnetic activity (that is, K_p variations between 1 and 2), MCILWAIN (1974) constructed an empirical electric field model from ATS 5 satellite data that includes both magnetospheric and corotational electric field components. Using this so-called E3H model for the electric field (E) and the associated M2 model for the magnetic field (B), Fig. 1 shows the equatorial drift paths of three plasma elements initially located at 8, 6, and 3 R_E (Earth radii) in the dusk sector. Since plasma interchange motion resulting from gravitational, centrifugal, and inertial forces is not included, the drift velocity of these cold plasma elements is given by $E \times B/B^2$. Also, since the E and B fields do not depend on time, the drift paths of these elements are closed curves that coincide with the equipotentials of the background (external) E-field distribution. The successive positions of the plasma elements are given every 30 min of Universal Time (UT) along the paths. The positions are indicated by dots for the innermost path and by the symbols ($\square$, +) for both of the other two paths. Note that for the two outer paths, the symbol changes after midnight. Since the distance between successive 30 min positions is inversely proportional to the convection speed, an inspection of the two outer trajectories indicates that these plasma elements slow down in the dusk sector and accelerate after midnight.

If the MHD approximation is valid, as assumed in the case shown in Fig. 1, plasma elements with an excess density (as well as those with a depressed density, or bubbles) are forced to follow the same

drift path as the background plasma elements. Indeed, because of the infinite conductivity assumed in ideal MHD theory, the electric field inside a plasma density enhancement (or bubble) cannot be different from the background E-field outside this element. Therefore, conservation of magnetic flux indicates that the equatorial cross-section (S_{eq}) of a flux tube of plasma varies inversely with the equatorial magnetic field intensity (B_{eq}),

$$S_{eq}(L) \propto B_{eq}^{-1}. \tag{1}$$

To show the change in equatorial cross-section as the plasma flux tubes follow their convection paths, the sizes of the symbols in Fig. 1 are drawn in proportion to S_{eq}.

As a consequence of the dawn–dusk asymmetry of the drift paths, the cross-section of a given plasma element shrinks when it drifts into a region of higher magnetic field strength, that is, when it drifts closer to the Earth. During this adiabatic contraction, the plasma density and temperature increase. Conversely, when the plasma element drifts away from the Earth toward regions of lower magnetic field, the plasma density and temperature decrease. The variation in the plasma density is given by

$$n_{eq}(L) \propto V^{-1}(L) \tag{2}$$

where $V(L)$ is the volume of the plasma element.

When K_p is less than 2, corotation prevails at least up to $L = 2$. Therefore, the inner plasma element drifts around the Earth along an almost circular trajectory at $L = 3$ in a period of 24 h. The second plasma element orbiting at intermediate radial distances ($L = 4.5$–6) circulates around the Earth in a 32-h period, while the outer plasma element ($L = 5$–8) takes 34 h to complete a revolution. Note that the inner trajectory is nearly circular and that the dawn–dusk asymmetry in the drift paths increases further from the Earth. The consequences of this dawn–dusk asymmetry have been discussed by LEMAIRE (1985) in connection with the equatorial density (n_{eq}), the flux tube content (NT), the average ion temperature, and the ion temperature anisotropy ($T_\perp/T_\parallel$).

2.2. *Equatorial densities in drifting and refilling flux tubes*

The dawn–dusk asymmetry in the drift paths of convecting plasmaspheric flux tubes has an important effect on the diurnal variation of n_{eq} during flux tube refilling conditions. To show this, it is necessary to adopt a numerical model to describe the refilling process. In this regard, it should be noted that 'plasmasphere refilling' following geomagnetic substorms is still a controversial subject. Numerous models have been used over the years, including diffusion (subsonic) models, single-fluid hydrodynamic (supersonic) models, multi-fluid hydrodynamic models, generalized transport models and kinetic models (cf. BANKS *et al.*, 1971; BAILEY *et al.*, 1978; KHAZANOV *et al.*, 1984; GUITER *et al.*, 1991; RASMUSSEN and SCHUNK, 1990; WILSON *et al.*, 1990; and references therein). Different results have been obtained, depending on what model was adopted, what physical processes were included, and what boundary conditions were assumed.

For our purposes it is sufficient to consider a simple refilling scenario for the flux tubes following the three drift paths in Fig. 1. Initially ($t = 0$), the flux tubes are located in the dusk local time sector ($\phi = 1800$ LT) at $L = 8$, 6 and 3 for flux tubes a, b and c, respectively. The initial plasma density on these flux tubes is low (nearly empty flux tubes). Subsequently ($t > 0$), the flux tubes begin to drift and refill via an upward ionization flux (F) from the ionosphere during a prolonged period of quiet magnetic conditions. The adopted ionization flux varies with time as n_{eq} increases and is given by

$$F = F_{max}[n_{eq}^{DE} - n_{eq}]/n_{eq} \tag{3}$$

where $n_{eq}^{DE}(L, \phi)$ is the saturation equatorial density for diffusive equilibrium (DE) at an equatorial distance L and local time ϕ, and $n_{eq}(L, \phi, t)$ is the actual equatorial density in the flux tube at the same L and ϕ at time t. The factor F_{max} in equation (3) is the maximum or limiting polar wind flux (LEMAIRE, 1972),

$$F_{max} = N_o(kT_o/2\pi M)^{1/2} \tag{4}$$

where k is Boltzmann's constant, M is the H^+ mass, and N_o and T_o are the H^+ density and temperature at the ion-exobase altitude (≈ 1000 km), respectively. For $N_o = 10^3$ cm^{-3} and $T_o = 3000$ K, $F_{max} = 2 \times 10^8$ cm^{-2} s^{-1}. This value is used in our calculations and is in agreement with the observed rate of increase in daytime tube content, as determined from whistler observations (PARK, 1970).

Figure 2a–c shows, respectively, the variations of $n_{eq}[L(t), \phi(t)]$ for the three refilling flux tubes convecting along the three drift paths illustrated in Fig. 1. The abscissa gives the local time $\phi(t)$ of the flux tube at Universal Time t. At the initial time ($t = 0$), the flux tubes are all located at $\phi_o = 1800$ LT, but at different equatorial distances ($L_o = 8$, 6 and 3). Their initial equatorial densities are, respectively, equal to 0.8 cm^{-3} for the outer flux tube (a), 2.5 cm^{-3} for the intermediate flux tube (b), and 41 cm^{-3} for the inner flux tube (c).

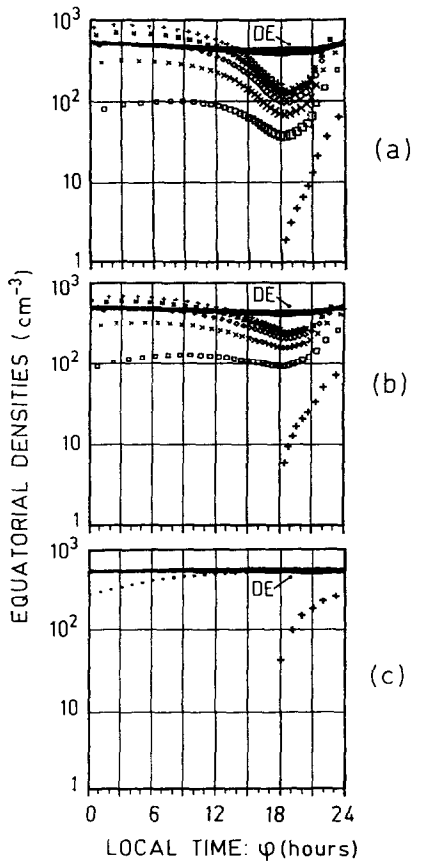

Fig. 2. Equatorial densities for three plasma elements drifting in the (E3H; M2) electric and magnetic field distributions along the trajectories illustrated in Fig. 1. The series of different symbols indicate the successive values of n_{eq} as a function of local time (ϕ) at 30 min intervals. The size of the symbols changes along the drift path to indicate the variation of the equatorial cross-section of the plasma element. The type of symbols changes when the plasma element traverses the meridional plane (ϕ = 0000, 2400, 4800 LT, ...). The solid line marked '*DE*' gives the equatorial density in a magnetic flux tube when Diffusive Equilibrium (*DE*) is achieved. The panels show the refilling rate that is superimposed on a large amplitude diurnal variation of n_{eq} for a plasma element whose initial (t = 0) equatorial density is (a) $n_{eq} = 0.8\,\mathrm{cm}^{-3}$ at $L = 8$ and ϕ = 1800 LT; (b) $n_{eq} = 2.5\,\mathrm{cm}^{-3}$ at $L = 6$ and ϕ = 1800 LT; and (c) $n_{eq} = 41\,\mathrm{cm}^{-3}$ at $L = 3$ and ϕ = 1800 LT (after LEMAIRE, 1985).

When the plasma flux tubes move along the drift paths shown in Fig. 1, the local time angle $\phi(t)$ increases continuously with time. The equatorial density $n_{eq}[\phi(t)]$ increases exponentially both with Universal Time and with local time $\phi(t)$, as shown in Fig. 2a–c. Note that the different curves shown in each panel illustrate the build-up of the equatorial density during successive revolutions around the Earth; that is, after each successive 24 h local time period. As in Fig. 1, the variable size of the symbols indicates the variation of the equatorial cross-section of the plasma flux tube, assuming that magnetic flux is conserved. The larger the size of these symbols, the larger is the cross-section of the flux tube.

The equatorial densities corresponding to Diffusive Equilibrium (n_{eq}^{DE}) are given by the solid curves near 450 cm^{-3}. This is the equatorial density when the flux tubes become saturated; that is, when all trapped particles are in thermal equilibrium with those emerging from the ionosphere. When n_{eq} exceeds n_{eq}^{DE}, the field-aligned flux given by equation (3) becomes negative; plasma stored in the plasmasphere is then dumped into the ionosphere. This is precisely what happens between 0000 and 1200 LT for the outer flux tube (*a*) after several days of refilling (four revolutions around the Earth). The same happens even earlier to the intermediate flux tube (*b*).

2.3. *Refilling times*

Figure 2a–c shows that the outer flux tube (*a*), which drifts out to 8 R_E, takes 7 days to reach diffusive equilibrium (i.e., 5 revolutions around the Earth). The flux tube circulating around the Earth between $L = 4.5$ and 6 takes 5 days to refill (or 4 revolutions), while the inner flux tube drifting at $L = 3$ takes only 24 h (i.e., 1 revolution) to reach diffusive equilibrium. Therefore, a flux tube at $L = 4$ would take only 2.5 days to completely refill and reach a state of diffusive equilibrium.

The refilling times deduced by PARK (1970, 1974) from whistler observations are, however, generally longer than these calculated times. For instance, according to Park's observations 'an 'empty' tube of force at $L = 4$ requires about 5 days to reach the monthly median value, and even after 8 days of quiet conditions it continues to fill' (PARK, 1970). In other words, the observations show that after 8 days a flux tube at $L = 4$ is not yet saturated, and that after 5 days its equatorial density (n_{eq}) only reaches the monthly median value, which is significantly smaller than n_{eq}^{DE}. On the other hand, our numerical simulations indicate that in about 2.5 days a flux tube at $L = 4$ should already be saturated (that is, $n_{eq} = n_{eq}^{DE}$).

There could be several reasons why our calculated refilling time for an $L = 4$ flux tube differs from that deduced by PARK (1970, 1974). First, substorms could deplete the flux tube while it is refilling, but since we are considering a prolonged period of quiet magnetic conditions this is not possible. Next, the limiting polar wind flux (F_{max}) from the ionosphere exhibits a diurnal variation owing to its dependence on N_o and T_o, which

was not included in our calculations. However, this diurnal variation would increase the refilling time by about a factor of two (5 days), which is still too short compared with the measurements (LEMAIRE, 1985). Finally, it is possible that some mechanism (electrostatic waves, counterstreaming flows, etc.) not included in our calculations acts to slow down the refilling process. Unfortunately, as noted earlier, plasmasphere refilling is still a controversial subject and the available measurements are not sufficient to eliminate any of the proposed mechanisms.

The discrepancy between our simulation results and the observations of Park can be resolved if it is assumed that in addition to corotation–convection around the Earth all plasma elements also have a small outward expansion velocity. In other words, instead of circulating along closed streamlines (as illustrated in Fig. 1) all plasma elements spiral away from the Earth along open drift paths. In this case, all drift paths would be open, and the volume of the plasma elements would continuously expand as would their equatorial cross-section. It definitely takes more time to refill a flux tube whose volume continuously expands than to refill one which always circulates along the same closed drift path, as in Fig. 1. Therefore, a slow radial expansion of the thermal plasma both inside and outside the plasmasphere could explain the longer refilling times observed by PARK (1970). In a steady-state situation, this slow (subsonic) expansion or 'plasmaspheric wind' would yield a plasma loss rate that is equal to the imbalance between what flows up into the plasmasphere from the dayside ionosphere and what flows back down into the nightside ionosphere.

The above arguments show how the existence of a plasmaspheric wind, which to some extent is similar to the solar corona subsonic expansion, can explain the relatively long refilling times observed by PARK (1970).

2.4. *Maximum equatorial densities*

From Fig. 2 it can be seen that the equatorial density in the drifting flux tubes is generally smaller in the afternoon and dusk sectors than in the pre-noon sector. The amplitude of this diurnal variation superimposed on the slow refilling of the plasma flux tubes is much larger along the outer ($L = 8$) drift path than along the inner ($L = 3$) drift path. This is a consequence of the large dawn–dusk asymmetry of the convection streamlines in the outer plasmasphere. Therefore, the largest diurnal variations of equatorial densities are expected in the outer regions of the plasmasphere.

As a result of the flux tube contraction in the post-dusk sector, n_{eq} can eventually exceed n_{eq}^{DE}. For instance, Fig. 2a shows that after 5 successive revolutions an equatorial density larger than 930 cm^{-3} is obtained at $L = 4.8$ when the plasma element is in the midnight local time sector. On the contrary, at dusk (1800 LT), where the trajectory has its maximum extent, the minimum equatorial density does not drop below 134 cm^{-3} at $L = 8$. Both the value of the post-midnight maximum (930 cm^{-3} at $L = 4.8$) and the value of the dusk minimum (134 cm^{-3} at $L = 8$) are generally larger than the observed values by a factor of 3 or 4 (CHAPPELL *et al.*, 1970a, b; PARK *et al.*, 1978).

A way to explain the lower equatorial densities that have been measured in the outer plasmasphere is again to assume that the plasmasphere continuously expands and that this continuous radial expansion forms a subsonic 'plasmaspheric wind' similar to the coronal expansion. A consequence of such a plasmaspheric wind is that during quiet magnetic conditions the equatorial density would decrease faster with L than that corresponding to diffusive equilibrium.

2.5. *Equatorial density gradient*

When the flux tube refilling rate is assumed to be zero or relatively small and the plasmaspheric wind velocity (v_{eq}) is assumed to be uniform (i.e., independent of L), the equatorial density distribution, $n_{eq}(L)$, in such an expanding plasmasphere varies as L^{-4} (i.e., as the inverse of the flux tube volume)

$$n_{eq}(L) \approx D/L^4. \tag{5}$$

This results from the continuity equation and corresponds to the conservation of total particle flux in a dipole magnetic field distribution when v_{eq} is a constant and independent of L (see GREBOWSKY, 1970). Such a characteristic L^{-4} equatorial density profile is often observed in the outer plasmasphere (CARPENTER, 1963; CHAPPELL *et al.*, 1970a, b; KOWALKOWSKI and LEMAIRE, 1979; ANDERSON, 1990).

Figure 3 shows a clear example of an L^{-4} density variation taken from OGO-5 observations available at NSSDC. The L^{-4} equatorial density distribution exists inside the plasmasphere for $L < 4.5$. The data were taken on 5 January 1969 after a series of very quiet days. The daily averages of K_p and A_p on that day and on the four preceding days are given in Table 1. The data shown in Fig. 3 were taken in the pre-midnight local time sector (21–23 LT) when K_p was equal to 2−. The constant (D) in equation (5) can be determined empirically from the observations, which show that the background plasma

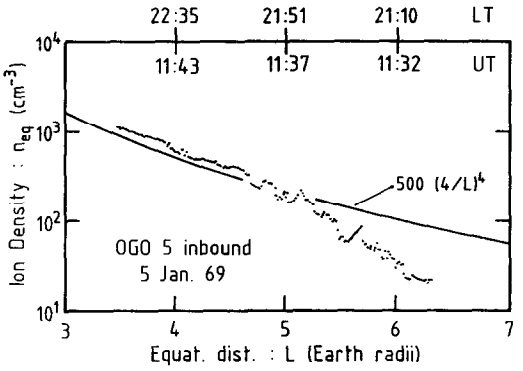

Fig. 3. Equatorial ion densities $n_{eq}(L)$ deduced from OGO-5 observations along the inbound part of its trajectory on 5 January 1969. These observations were made in the 21–23 LT sector after a prolonged period of quiet geomagnetic conditions. The solid line shows the slope corresponding to an L^{-4} density profile.

density at $L = 4$ is often equal to 500 ions/cm^3. With this value for the plasma density, equation (5) yields $D = 1.28 \times 10^5$ ions/cm^3.

2.6. *Reduced expansion rates*

Equation (5) was derived from the steady-state continuity equation assuming that the refilling rate was zero or small compared with the expansion rate. When this condition is not satisfied, the equatorial density decreases more slowly with L than the L^{-4} dependence in equation (5). In this case the equatorial density profile tends to approach, in an asymptotic manner, the diffusive equilibrium density profile, which is much flatter (LEMAIRE, 1989a).

Figure 4 shows an equatorial density profile taken in the pre-noon local time sector after prolonged quiet geomagnetic conditions (see Table 1). This figure displays a plasmaspheric density slope that is smaller than that corresponding to the L^{-4} profile. The distribution of $n_{eq}(L)$ is between the L^{-4} profile and the barometric (or diffusive equilibrium) profile, which correspond to large and small expansion rates, respectively.

Table 1. Geomagnetic activity conditions

Day of 1969	K_p								$\bar{K}_p$	$\bar{A}_p$
01	3−	1+	1+	3−	2+	2o	1+	2o	1.96	8
02	0+	2+	0+	1−	1+	1+	0+	0o	0.83	4
03	0o	0o	0o	0+	1o	0o	0+	0+	0.25	1
04	0o	0+	0o	1−	2−	0+	1+	1o	0.66	3
05	1o	2−	0+	1−	1−	0+	0o	1−	6.66	3
Day of 1968										
294	2+	1+	3−	3−	2−	2−	1−	0+	1.66	7
295	0o	0o	0+	1−	0+	1o	0+	0+	0.37	2
296	0o	0o	0o	0o	1−	0+	0+	0+	0.21	1
297	0o	0o	0+	0+	1−	1+	2−	1o	0.66	3
298	1o	1o	0+	1o	1+	3−	4−	1+	1.54	7

2.7. *Non-uniform expansion velocity*

Equation (5) was also derived from the continuity equation assuming that the expansion velocity, $v_{eq}(L)$ was independent of L. However, this is not necessarily the case. When $v_{eq}(L)$ increases with L in both the plasmapause region and outside the plasmasphere, conservation of mass implies that the equatorial density $n_{eq}(L)$ decreases more rapidly with L than L^{-4}. This is, for example, the case in Fig. 3 for $L > 4.5$, where the density gradient is steeper than at lower L-values.

It should be noted here that a sharp 'knee' is not present in the equatorial density profiles shown in Figs 3 and 4. It is generally after substorm associated enhancements of geomagnetic activity, during which the convection electric field is enhanced, that a sharp 'knee' forms in $n_{eq}(L)$ at the plasmapause.

2.8. *Absence of density 'knee'*

Note that the absence of steep density gradients after prolonged quiet conditions, as in Figs 3 and 4, is contrary to the predictions of ideal MHD theory for the formation of the plasmapause. Indeed, during prolonged ideally quiet conditions, a well-developed and stationary density 'knee' should exist along the 'Last Closed Equipotential' (LCE) of the magnetospheric convection electric field. Also, under quiet conditions the position of the LCE should be almost independent of time according to MHD theory.

The absence of sharp density 'knees' in Figs 3 and 4, leads, therefore, to the conclusion that not even during quiet conditions, when the magnetospheric convection electric field is time independent, can the plasmapause be considered to be coincident with the 'Last Closed Equipotential' of a postulated E-field distribution. It should be noted here that there is no compelling observational reason to assume that the equipotential lines are closed curves inside the plasmasphere, not even for a stationary model. Indeed, when the plasmasphere has a slow outward drift velocity in addition to the much larger corotation drift, as is the case for the inner solar corona plasma, all equipotential lines would be 'open' spirals instead of closed curves. Of course, in this case there is no 'stag-

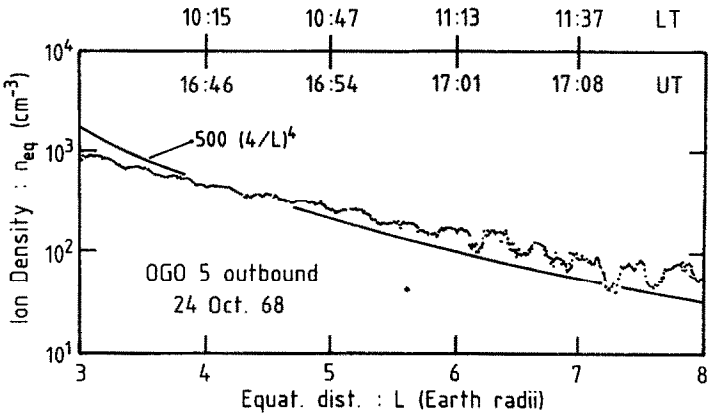

Fig. 4. Equatorial ion densities $n_{eq}(L)$ deduced from OGO-5 observations along the outbound part of its trajectory on 24 October 1968. These observations were made in the 10–11 LT sector after a prolonged period of quiet geomagnetic conditions. The solid line shows the slope corresponding to an L^{-4} density profile.

nation point' as postulated in all magnetospheric E-field distributions considered since 1966–1967.

2.9. *Additional observational evidence for the existence of a plasmaspheric wind*

Evidence for a continuous outward plasma expansion has been presented by TITHERIDGE (1976b). Figure 5 shows the latitude region over which an upward ionization flux was deduced to exist by examining topside plasma scale heights. In the shaded region above geomagnetic latitudes labelled A, the O^+/H^+ transition altitude h_T (where the H^+ density is larger than the O^+ density) is higher than the altitudes where chemical equilibrium prevails at all local times. Since this implies an upward ionization flow, it can be concluded that along all field lines in the plasmasphere for $L \geqslant 1.7$–2 the light ion flux is upward at all local times. A continuous and extensive upflow of this nature must be balanced by a plasma flow across geomagnetic field lines via a plasmaspheric wind and/or a substorm induced peeling off of the plasmasphere. Although the latter mechanism does operate, the substorms had to be frequent and the effects had to penetrate down to $L \approx 1.7$–2 in order to explain the observations in Fig. 5. Therefore, we conclude that the observations support our hypothesis of a plasmaspheric wind that is similar to the subsonic expansion of the inner corona of the Sun.

PARK (1970) has also shown from whistler observations that under quiet geomagnetic conditions the observed rate of increase in daytime flux tube content yields an upward flux of 3×10^8 electrons cm^{-2} s^{-1} at 1000 km altitude. This value is larger than the downward flux necessary to maintain the nocturnal ionosphere (that is, 1.5×10^8 electrons cm^{-2} s^{-1}). Since there are more ions flowing upward into the plasmasphere during the day than returning to the ionosphere during the night, we again conclude that there should be a continuous plasmaspheric wind carrying light ions across closed magnetic field lines from the inner plasmasphere to the outer regions of the magnetosphere. In addition to this slow subsonic expansion, the plasmasphere is peeled off, from time to time, in a more catastrophic manner via magnetospheric substorms (i.e., when geomagnetic activity is enhanced). Under disturbed conditions, large pieces of the slowly expanding plasmasphere break away from the main cold plasma body (LEMAIRE, 1983, 1985).

3. FACTORS CONTROLLING THE PLASMASPHERIC WIND

3.1. *Driving force*

As in the case of the solar corona, the continuous expansion of the plasma results from an imbalance between the total plasma pressure gradient ($\nabla[p + B^2/2\mu_0]$) and the gravitational force ($\rho \mathbf{g}$). The larger the difference between these two vectors, the larger is the inertial force ($\rho \partial \mathbf{v}/\partial t + \rho(\mathbf{v} \cdot \nabla)\mathbf{v}$). This force per unit volume, resulting from a non-steady state and/or a non-uniform distribution of the expansion velocity $\mathbf{v}$, vanishes when diffusive equilibrium is obtained in the plasmasphere ($\mathbf{v} = 0$) or when $\mathbf{v}$ is constant and independent of L (uniform translation). However, large plasma pressure gradients will drive a continuous outward flow of plasma (i.e., a plasmaspheric wind).

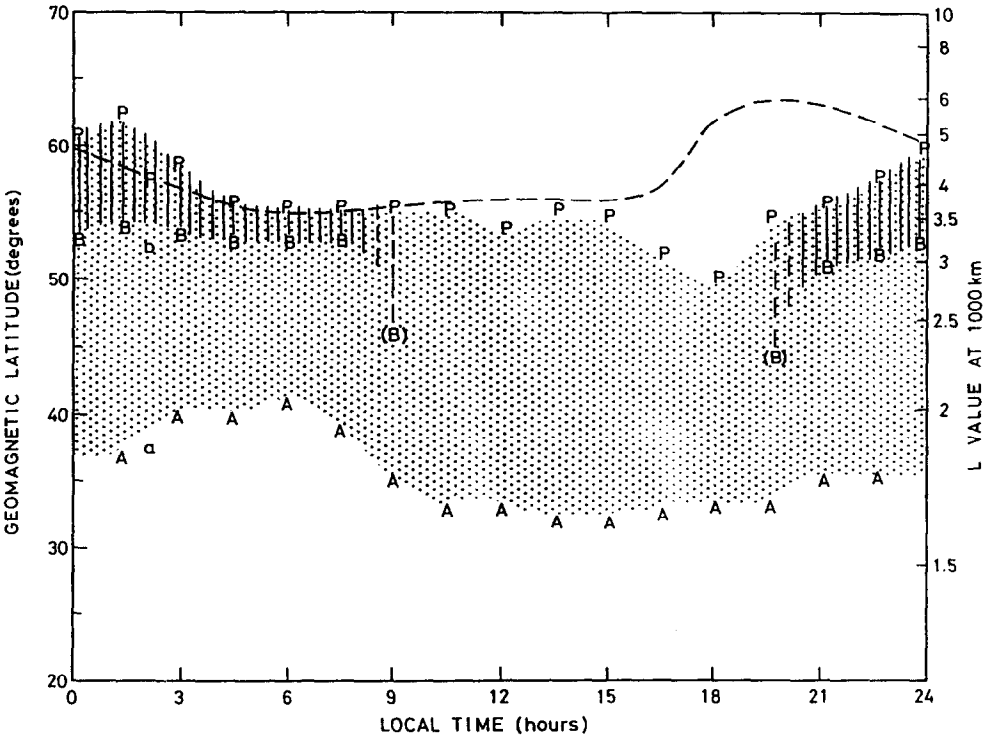

Fig. 5. Geomagnetic latitudes where upward H^+ fluxes exist. The dashed line shows the local time dependence of the equatorial plasmapause position as determined from whistler observations. The *P*s correspond to the low altitude projection of the plasmapause, as identified by the peak in the plasma temperature distribution as a function of geomagnetic latitude. The shaded zone between the *A*s and *P*s corresponds to a region of upward ionization flow, with a field-aligned flux that increases between latitudes *A* and *B*. *B* is the lowest latitude where the observed O^+/H^+ transition heights (h_T) indicate that the upward ionization flux equals the limiting polar wind flux. In the hatched zones between latitudes *B* and *P*, a limiting upward polar wind flux of H^+ ions is inferred from the high altitude of h_T (after TITHERIDGE, 1976b).

At large radial distances, where the gravitational acceleration becomes small and where it is dominated by the pseudo-centrifugal force, diffusive equilibrium can only be achieved when the plasma pressure gradient is zero or positive. A positive pressure gradient implies a pressure that increases indefinitely with radial distance (a non-zero pressure at infinity). However, observations consistently indicate that $n_{eq}(L)$ generally decreases as a function of L. Also, the plasma pressure decreases more steeply with L than in the case corresponding to diffusive equilibrium. The observations, therefore, indicate that the kinetic plasma pressure is zero or small at infinity. Hence, one is led to conclude, like PARKER (1958) did to infer the existence of the solar wind, that the plasma pressure at large distances in the magnetosphere is not high enough to maintain the plasmasphere in hydrostatic (magnetostatic) equilibrium, and hence, that there is a plasmaspheric wind.

3.2. *Drag force; maximum interchange velocity*

It has been emphasized by LEMAIRE (1976, 1985) that the bulk velocity of a magnetospheric plasma element is not only determined by *local plasma conditions* (i.e., gravitational, pressure gradient and centrifugal forces), but by non-local conditions as well. Examples are the electrical conductivity in the distant ionospheric layers in the case of plasma elements moving in or into the magnetosphere and the walls of a vacuum tank in the case of plasmoids moving across laboratory magnetic fields (see LEMAIRE, 1989b).

Although these non-local conditions (for example, the value of the ionospheric Pedersen conductivity along the magnetic field lines across which the plasma

is drifting) are ignored in ideal (as well as non-ideal) MHD models of magnetospheric convection, they must be taken into account in future realistic descriptions and models. This is also true for the plasmaspheric wind discussed in this paper. In other words, the outward expansion rate of the plasma both inside the plasmasphere and in the plasmapause region is not only determined by the external driving forces (gravitational, centrifugal, inertial forces, etc.), which appear in the momentum equation, but the maximum value of the expansion velocity in the magnetosphere is eventually controlled by the value of the integrated Pedersen conductivity (Σ_p). More specifically, $v_{eq}(L)$ is inversely proportional to Σ_p (see WALBRIDGE, 1967; LEMAIRE, 1985; SOUTHWOOD and KIVELSON, 1987, 1989).

In the sunlit hemisphere, where the ionosphere is a good electrical conductor and Σ_p is large, the maximum plasma interchange velocity v_{max} is reduced compared with its value in the nightside ionosphere, where Σ_p is relatively small. This means that in regions of the plasmasphere linked to the dayside ionosphere the magnetospheric convection electric field imposed by the local magnetospheric plasma distribution [$\mathbf{E} = -(\nabla p_e)/n_e e$] is short-circuited by the low resistivity in the ionospheric E-region. This implies that the ionospheric conductivity regulates the electric field and convection velocity in the dayside inner magnetosphere. Consequently, the magnetospheric plasma density (n_e) and pressure (p_e) distributions have to adjust to the conditions imposed from below by the highly conducting ionosphere.

The same should also be true for the nightside plasmasphere, which is linked to ionospheric regions where the maximum ionospheric Pedersen conductivity is relatively small (see BREKKE and HALL, 1988). However, in this case, the relaxation time for the magnetospheric plasma to adjust to the ionospheric conditions is significantly longer (proportional to Σp^{-1}) and, hence, the maximum convection velocity (or plasma interchange velocity, v_{max}) is significantly larger. Therefore, one expects that the plasmaspheric expansion velocity (i.e., the maximum plasma interchange velocity) is lower in the dayside local time sector than in the night-time sector.

This conclusion is supported by the observations displayed in Figs 3 and 4. In Fig. 3, which corresponds to night-time conditions, $\Sigma_p(L)$ must be small (0.1–1 mho depending on the latitude; that is, on L) and $v_{eq}(L)$ must be relatively large. The expansion rate might then be more important than the refilling rate of flux tubes by evaporation from the nightside ionosphere. Under these conditions, we argued above that the L^{-4} equatorial density profile [equation (5)] would be applicable, at least when $v_{eq}(L)$ is uniform (independent of L). Since $\Sigma p(L)$ is nearly independent of L at low and mid-latitudes, it may be inferred that $v_{eq}(L)$ is also approximately independent of L and that $n_{eq}(L)$ varies as L^{-4} for $L < 4.5$.

Above, we attributed the larger density slope beyond $L = 4.5$ in Fig. 3 to an increase of the expansion velocity $v_{eq}(L)$ as a function of L. This increase of the interchange velocity with L may be accounted for by the decrease of Σ_p as a function of invariant latitude.

On the contrary, in Fig. 4 the density slope is smaller than that of the L^{-4} profile. We explained this by noting that in this case the expansion rate of the plasmasphere (the plasmaspheric wind interchange velocity) is relatively small compared with the refilling rate via evaporation from the ionosphere. This explanation is well supported by the fact that the observations reported in Fig. 4 were obtained in the dayside local time sector (10–11 LT), which is where the plasmaspheric refilling rate is large because of the large ionospheric plasma density and where the maximum outward plasmaspheric wind velocity is small because of the enhanced value of the integrated Pedersen conductivity in the sunlit ionosphere. Under these slow expansion rate conditions, the L^{-4} density profile will be offset by the process of refilling which tends to saturate flux tubes in a state of diffusive equilibrium. The density slope then tends to become smaller than that corresponding to the L^{-4} profile.

In conclusion, we interpret the relatively small density slope shown in Fig. 4 to be a direct consequence of the large plasma density in the dayside ionosphere, which yields a large plasmaspheric refilling flux and a large integrated Pedersen conductivity. These, in turn, yield a reduced plasmaspheric wind velocity in the dayside plasmasphere.

4. CONCLUSIONS

The plasmasphere is usually considered to be a reservoir of cold plasma that corotates with the ionosphere at low latitudes and that follows closed $\mathbf{E} \times \mathbf{B}$ drift paths at the latitudes where magnetospheric electric fields dominate. However, we have presented physical arguments and observational evidence that suggest the existence of a plasmaspheric wind. This slow (subsonic) expansion of the plasma away from the Earth implies that even during quiet geomagnetic conditions the streamlines are not 'closed'. The cold plasma elements slowly drift outwards from the inner plasmasphere to the plasmapause along open spiral curves. This large-scale and continuous expansion of

the plasmasphere is somewhat similar to the subsonic expansion of the inner solar corona. In this latter well-known case, there are no mathematical singularities in the equipotential distribution where $\mathbf{E} = 0$, that is, no stagnation points where $\mathbf{v} = 0$.

The slow plasmasphere expansion rate, which is governed by plasma interchange motion, is driven by an imbalance between pressure gradient, gravitational, centrifugal, and inertial forces. The expansion velocity is also controlled by the height-integrated Pedersen conductivity (Σ_p) of the ionosphere. The expansion rate and outward drift velocity are inversely proportional to Σ_p. From the local time dependence of Σ_p, we deduced that the plasmaspheric wind velocity should be reduced in the local noon sector and enhanced throughout the night. We also concluded that the plasmaspheric interchange velocity must be larger in the outer plasmasphere than in the inner plasmasphere, where $v_{eq}(L)$ is nearly independent of L. Furthermore, it should be noted that plasma interchange motion is ignored in MHD convection models where non-local boundary conditions in the ionosphere are not taken into account.

Our overall conclusions are well supported by a series of whistler observations by PARK (1970, 1974), PARK *et al.* (1978), and CARPENTER (1963) as well as by satellite observations by CHAPPELL *et al.* (1970a, b), TITHERIDGE (1976a, b) and ANDERSON (1990).

Acknowledgements—This work has been supported in part by NASA grant NAG5-1484 to Utah State University.

REFERENCES

ANDERSON K. 1990 Dynamical plasma parameters and processes deduced from plasmaspheric wave observations. Proceedings of Workshop on Plasmasphere Refilling, University of Alabama, Huntsville, 15–16 October.

BAILEY G. J., MOFFETT R. J., HANSON W. B. and SANATANI S. 1973 *J. geophys. Res.* **78**, 5597.

BAILEY G. J., MOFFETT R. J. and MURPHY J. A. 1977 *Planet. Space Sci.* **25**, 967.

BAILEY G. J., MOFFETT R. J. and MURPHY J. A. 1978 *Planet. Space Sci.* **26**, 753.

BANKS P. M., NAGY A. F. and AXFORD W. I. 1971 *Planet. Space Sci.* **19**, 1053.

BREKKE A. and HALL C. 1988 *Ann. Geophysicae* **6**, 361.

BRICE N. M. 1967 *J. geophys. Res.* **72**, 5193.

CARPENTER D. L. 1963 *J. geophys. Res.* **68**, 1675.

CARPENTER D. L. 1970 *J. geophys. Res.* **75**, 3837.

CARPENTER D. L. and PARK C. G. 1973 *Rev. Geophys. Space Phys.* **11**, 133.

CHAPPELL C. R. 1972 *Rev. Geophys. Space Phys.* **10**, 951.

CHAPPELL C. R., HARRIS K. K. and SHARP G. W. 1970a *J. geophys. Res.* **75**, 50.

CHAPPELL C. R., HARRIS K. K. and SHARP G. W. 1970b *J. geophys. Res.* **75**, 3848.

GREBOWSKY J. M. 1970 *Radio Sci.* **5**, 601.

GREBOWSKY J. M. and CHEN A. J. 1976 *Planet. Space Sci.* **24**, 689.

GRINGAUZ K. I. 1963 *Planet. Space Sci.* **11**, 281.

GUITER S. M., GOMBOSI T. I. and RASMUSSEN C. E. 1991 *Geophys. Res. Lett.* **18**, 813.

KHAZANOV G. V., KOEN M. A., KONIKOV Y. V. and SIDOROV I. M. 1984 *Planet. Space Sci.* **32**, 585.

KOWALKOWSKI L. and LEMAIRE J. 1979 *Acad. Royale Belgique* **65**, 159.

LEMAIRE J. 1972 *J. atmos. terr. Phys.* **34**, 1647.

LEMAIRE J. 1976 *Planet. Space Sci.* **24**, 975.

LEMAIRE J. 1983 Formation and deformation of the plasmapause. Video-montage, Institut d'Aéronomie Spatiale de Belgique, Bruxelles.

LEMAIRE J. 1985 Frontiers of the plasmasphere. Thèse d'Agrégation de l'Enseignement Supérieur à l'Université Catholique de Louvain, June 1985, Ed. Cabray. *Aeronomica Acta A*, 298.

LEMAIRE J. 1989a *Phys. Fluids B* **1**, 1519.

LEMAIRE J. 1989b Impulsive penetration of solar wind plasma irregularities into the magnetosphere: relevant laboratory experiments. In *Electromagnetic Coupling in the Polar Clefts and Caps*, SANDHOLT P. E. and EGELAND A. (eds). Kluwer, Dordrecht (series C: Vol. 278, p. 27).

MAYR H. G., FONTHEIM E. G., BRACE L. H., BRINTON H. C. and TAYLOR H. A. JR 1972 *J. atmos. terr. Phys.* **34**, 1659.

McIlwain C. E.	1974	Substorm injection boundaries. In *Magnetospheric Physics*, McCormic B. M. (ed.), pp. 143–154. D. Reidel, Dordrecht.
Moffett R. J. and Murphy J. A.	1973	*Planet. Space Sci.* **21,** 43.
Murphy J. A., Bailey G. J. and Moffett R. J.	1976	*J. atmos. terr. Phys.* **38,** 351.
Murphy J. A., Bailey G. J. and Moffett R. J.	1980	*J. geophys. Res.* **85,** 1979.
Nishida A.	1966	*J. geophys. Res.* **71,** 5669.
Park C. G.	1970	*J. geophys. Res.* **75,** 4249.
Park C. G.	1974	*J. geophys. Res.* **79,** 169.
Park C. G., Carpenter D. L. and Wiggin D. B.	1978	*J. geophys. Res.* **83,** 3137.
Parker E. N.	1958	*Astrophys. J.* **128,** 664.
Rasmussen C. E. and Schunk R. W.	1988	*J. geophys. Res.* **93,** 14557.
Rasmussen C. E. and Schunk R. W.	1990	*J. geophys. Res.* **95,** 6133.
Richards P. G., Schunk R. W. and Sojka J. J.	1983	*J. geophys. Res.* **88,** 7879.
Richards P. G. and Torr D. G.	1986	*J. geophys. Res.* **91,** 9017.
Schulz M. and Koons H. C.	1972	*J. geophys. Res.* **77,** 248.
Singh N., Schunk R. W. and Thiemann H.	1986	*J. geophys. Res.* **91,** 13433.
Southwood D. J. and Kivelson M. G.	1987	*J. geophys. Res.* **92,** 109.
Southwood D. J. and Kivelson M. G.	1989	*J. geophys. Res.* **94,** 299.
Titheridge J. E.	1976a	*J. atmos. terr. Phys.* **38,** 623.
Titheridge J. E.	1976b	*J. geophys. Res.* **81,** 3227.
Walbridge E.	1967	*J. geophys. Res.* **72,** 5213.
Wilson G. R., Ho C. W., Horwitz J. L., Singh N. and Moore T. E.	1990	*Geophys. Res. Lett.* **17,** 263.
Young E. R., Torr D. G., Richards P. and Nagy A. F.	1980	*Planet. Space Sci.* **28,** 881.